THE JOURNAL OF BIOLOGICAL CHEMISTRY
Vol. 279, No. 43, Issue of October 22, pp. 44812–44816, 2004
Printed in U.S.A.

The Structure of the N-terminal Region of Murine Skeletal Muscle α-Dystroglycan Discloses a Modular Architecture*[S]

Received for publication, July 27, 2004, and in revised form, August 18, 2004
Published, JBC Papers in Press, August 23, 2004, DOI 10.1074/jbc.C400353200

Damir Bozic‡§, Francesca Sciandra¶, Doriano Lamba‖, and Andrea Brancaccio¶**

*From the ‡Biochemisches Institut der Universität Zürich, Zürich 8044, Switzerland, the ¶CNR-Istituto di Chimica del Riconoscimento Molecolare, c/o Istituto di Biochimica e Biochimica Clinica, Università Cattolica del S. Cuore Roma, I-00168 Rome, Italy, the ‖Consiglio Nazionale delle Ricerche, Istituto di Cristallografia, Unità Staccata di Trieste, Area Science Park, I-34012 Trieste, Italy, and the **International Centre for Genetic Engineering and Biotechnology, Area Science Park, I-34012 Trieste, Italy*

Dystroglycan (DG) is a cell surface receptor consisting of two subunits: α-dystroglycan, extracellular and highly glycosylated, and β-dystroglycan, spanning the cell membrane. It is a pivotal member of the dystrophin-glycoprotein complex and is involved in a wide variety of important cellular processes such as the stabilization of the muscle fiber sarcolemma or the clustering of acetylcholine receptors. We report the 2.3-Å resolution crystal structure of the murine skeletal muscle N-terminal α-DG region, which confirms the presence of two autonomous domains; the first finally identified as an Ig-like and the second resembling ribosomal RNA-binding proteins. Solid-phase laminin binding assays show the occurrence of protein-protein type of interactions involving the Ig-like domain of α-DG.

Dystroglycan (DG)[1] (1), earlier also identified as cranin (2), is a type-1 transmembrane protein expressed in muscle as well as in a wide variety of other tissues (3). Vertebrate DG is transcribed as a single mRNA and translates into a 895-amino acid polypeptide (1). This precursor undergoes an early posttranslational cleavage with the release of the highly glycosylated peripheral membrane protein α-DG and the transmembrane subunit β-DG, both being targeted separately to the plasma membrane (4). The two subunits remain tightly associated via non-covalent interactions. In skeletal muscle, they form together with sarcoglycans, sarcospan, syntrophins, and dystrobrevins the dystrophin-glycoprotein complex (DGC). This complex links the extracellular matrix (ECM) with the actin cytoskeleton and provides stability to the muscle fiber sarcolemma against contractile forces (3).

Electron microscopy studies showed that the α-DG subunit is a 20–30-nm-long dumbbell-shaped molecule. It contains a central mucin-like part, comprising residues 315–485, and is flanked by two globular regions (5) (see supplemental Fig. 1). The interactions of α-DG with laminin G-like domains "LG," also called "LNS" (LG/LNS) domain-containing ECM molecules, is thought to mainly involve the carbohydrate moieties protruding from the α-DG mucin-like region and the protein epitopes of LG/LNS domains (6, 7).

DG gene knock-out mice (8) show premature lethality, indicating that DG plays a crucial role during early embryonic development prior to myogenesis, muscle basement membrane formation, or stabilization. Accordingly, no natural genetic defects have been found in the highly conserved DG gene in living individuals so far, but genetic abnormalities in DG binding partners like laminin-2 or dystrophin as well as in any of the members of the sarcoglycan complex cause severe muscular dystrophy phenotypes (3).

Furthermore, α-DG can act as a direct receptor for Arena viruses, including Lassa fever virus (9, 10), and in complex with laminin-2 as a Schwan cell receptor for *Mycobacterium leprae*, the causative organism of leprosy infection (11). The amino acids 169–408 of α-DG contain an essential binding site for the entry of Arena viruses via its GP1 envelope protein (12).

The involvement of DG in this broad range of pathological situations makes it attractive for structural and functional studies aimed to define the molecular basis for the recognition of the binding partners in the DGC. The crystal structure of the murine α-DG fragment (50–313)R166H, corresponding to its N-terminal globular region, represents the first structural elucidation of a DG component. The structure is characterized by an N-terminal Ig-like domain and a C-terminal domain, whose fold resembles that of ribosomal RNA-binding proteins. The two domains are connected by a long and flexible linker. Solid-phase binding assays with the modular domain construct (28–313)R166H, not including the mucin-like region, as well as with each of the two separate domains, (28–168) and (168–313), respectively, pinpoint to the occurrence of some protein-protein interactions contributing to the laminin/α-DG interaction, as first reported by Hall *et al.* (13).

EXPERIMENTAL PROCEDURES

Crystallization and Data Collection—The murine α-DG(50–313)R166H DNA construct and the corresponding recombinant protein were prepared as described previously (14) using standard PCR protocols and appropriate primers. Crystals were grown at 4 °C by vapor diffusion sitting drops (3 μl + 3 μl) against a reservoir of 1 M sodium citrate/citric acid at pH 7.0 at a protein concentration of 7 mg ml^{-1}. To overcome the problem of twinning due to fast nucleation, the rate of crystal formation was slowed down using mineral oil seal covering the crystallization drop. For data collection the crystals were transferred to a solution containing 1.1 M sodium citrate/citric acid at pH 7.0 and 25% ethylene glycol. All data sets were collected using Cu*Kα* radiation from an Enraf-Nonius rotating-anode x-ray source and a MAR image-plate

* The costs of publication of this article were defrayed in part by the payment of page charges. This article must therefore be hereby marked "*advertisement*" in accordance with 18 U.S.C. Section 1734 solely to indicate this fact.

[S] The on-line version of this article (available at http://www.jbc.org) contains supplemental Figs. 1 and 2.

The atomic coordinates and structure factors (code 1U2C) have been deposited in the Protein Data Bank, Research Collaboratory for Structural Bioinformatics, Rutgers University, New Brunswick, NJ (http://www.rcsb.org/).

§ To whom correspondence should be addressed: Inst. for Biomedical Engineering, ETH Zürich, Moussonstr. 18 CH-8044 Zürich, Switzerland. Tel.: 41-1-632-45-86; Fax: 41-1-632-12-14; E-mail: damir.bozic@mat.ethz.ch.

[1] The abbreviations used are: DG, dystroglycan; DGC, dystrophin-glycoprotein complex; ECM, extracellular matrix; WB, washing buffer; BSA, bovine serum albumin.

TABLE I
Data statistics and refinement

The residue properties have an overall average G-factor of 0.3. In the Ramachandran plot 170 (89%) residues are within the core region and 21 residues (11%) in additionally allowed regions.

	Native 1	Native 2	Native 3[a]	Thiomer-salic acid	KI
Space group R3:	$\alpha = \beta = 90°$ $\gamma = 120°$				
a = , b = (Å)	71.4	71.4	71.4	71.4	71.6
c = (Å)	143.7	143.7	144.2	143.7	143.7
Maximum resolution (Å)	2.65	2.9	2.3	3.41	2.9
Measured reflections	64,525	25,105	63,864	22,330	28,135
Unique reflections	7812	5725	12143	4483	5489
$I/\sigma I$ (last shell)	9.4 (2.1)	10.2 (3.2)	13.1 (3.7)	4.9 (2.1)	9.1 (3.2)
Completeness (%)[b]	99.1 (96.9)	95.4 (94.3)	98.7 (98.1)	92.0 (93.6)	91.0 (89.2)
R_{merge} (%)	10.3 (44.5)	7.2 (18.2)	6.7 (35.6)	21.9 (40.0)	7.0 (15.0)
Twinning fraction[c]	0.237	0.103	0	0.278	0.06
Phasing power (isomorphous/anomalous)				2.3/0.68	1.8/0.9
Sites (used/present)[d]				5 (5)	7 (14)
R_{factor} (%)[b]			20.8 (23.8)		
No. of unique reflections $I \geq 0$			12,143		
R_{free} (%)[b]			26.2 (28.4)		
Resolution range (Å)			∞-2.3		
Root mean square deviation from ideality					
Bonds (Å)			0.007		
Angles (°)			1.200		
Average B-factors (Å^2)					
Main chain/main chain atoms			35.7/913		
Side chain/side chain atoms			36.6/778		
Solvent/solvent atoms			47.9/147		

[a] The data set was measured at the European Synchrotron Radiation Facility ID14-EH4. To overcome the twinning problem only small microcrystals were used. The data set was used exclusively for final refinement.
[b] Values in parentheses refer to the outermost shell.
[c] Twinning fraction calculated according to Yeates *et al*. (31).
[d] Sites present mean positions from a difference Fourier map using the final model and having peak heights >4 σ.

detector system with crystals flash frozen to 100 K in the nitrogen stream of an Oxford Cryosystems cooling device. The crystals belong to the space group R3 with unit cell constants $a = b = 71.4$ Å, $c = 144.2$ Å, $\alpha = \beta = 90°$, and $\gamma = 120°$. They have one molecule in the asymmetric unit with a calculated solvent content of 45%. All collected data were integrated and reduced with DENZO/SCALEPACK (15). Data collection and phasing statistics are given in Table I.

Structure Determination and Refinement—The crystal structure of murine α-DG(50–313)R166H was solved by SIRAS/MIR methods followed by restrained refinement with CNS_SOLVE (16) using all data to 2.3 Å (native 3). A bulk solvent correction was applied, and a 5% test set for the calculation of the R_{free} was used.

Only KI was found to be useful as a derivative for difference Patterson interpretation. Due to weak data quality combined with a high twinning fraction the thiomersalic acid heavy atom data set was not interpretable by difference Patterson methods but only useful for difference Fourier and cross phasing. Patterson map calculations were performed using CNS_SOLVE (16). Initial phasing was performed with MLPHARE followed by density modification using DM from the Collaborative Computational Project Number 4 suite (17). Final phasing was performed within SHARP (18).

Model building was performed with the programs MAIN (19) and O (20). When the high-resolution data set (native 3) became available, a round of simulated annealing from 5000 K was performed and the structure was refined to 2.3-Å resolution (Fig. 1). The refinement statistics are summarized in Table I.

Solid-phase Binding Assays—The full-length cDNA coding for murine dystroglycan was also used as template to generate both the α-DG N-terminal region (28–313)R166H and the separated domains (28–168)R166H and (168–313) by established PCR protocols. The recombinant proteins were expressed and purified as described elsewhere (21).

Murine laminin-1 (Sigma), α-DG(28–313)R166H, and domains α-DG(28–168) and α-DG(168–313) were biotinylated in 5 mM sodium phosphate buffer, pH 7.4, with 0.5 mg/ml sulfo-*N*-hydroxylsuccinimidobiotin with a molar ratio protein/biotin 1:10. The reactions were carried out for 30 min on ice. Biotinylated proteins were then dialyzed against 10 mM Tris/HCl, 150 mM NaCl, pH 7.4.

To assess the binding properties of recombinant α-DG fragments, solid-phase binding assays were performed as follows: 0.5 μg of murine laminin-1 (Sigma) were immobilized on microtiter plates in 50 mM $NaHCO_3$, pH 9.6, overnight at 4 °C. Plates were then washed with washing buffer (WB: phosphate-buffered saline, 0.005% Tween 20, 1.25 mM $CaCl_2$, 1 mM $MgCl_2$) and blocked with 3% BSA in WB. Wells were then incubated with increasing concentrations of biotinylated α-DG(28–313)R166H and of domains α-DG(28–168) and α-DG(168–313), in WB with 3% BSA for 3 h at room temperature. The biotinylated bound fraction was detected with alkaline phosphatase Vectastain AB Complex (Vector Laboratory) using a solution of *p*-nitrophenyl phosphate as substrate. Absorbance values, in triplicate, were recorded at 405 nm. Data were fitted using a "single class of equivalent binding sites" equation: $A_i = [A_{sat} \times (c/K_d+c)]$, where A_i represents the absorbance measured at increasing concentrations of ligand, K_d is the binding dissociation constant, c is the concentration of ligand, and A_{sat} is the absorbance at saturation. Data were normalized according to the equation (A_i/A_{sat}) and reported as fractional saturation (percent).

FIG. 1. **Stereo view of the final $2F_o - F_c$ density map contoured at the 1.8 σ level.** The region shows the hydrophobic core of the β-sheet of the second domain (178–303).

RESULTS AND DISCUSSION

Overall Structure—The murine α-DG N-terminal fragment shows an L-shaped modular domain architecture, and the presence of two autonomous domains is fully confirmed (14) (Fig. 2*A*). The first domain (Fig. 2, *A–C*) comprises residues 60–158 and belongs to the I-set of the Ig superfamily. The overall dimensions are 50 × 25 × 20 Å. The first β-sheet consists of the anti-parallel strands B, E, and D. The second β-sheet is formed by the strands A′, G, F, and C with strands A″ and G arranged in a parallel and G, F, and C in an anti-parallel fashion. Two

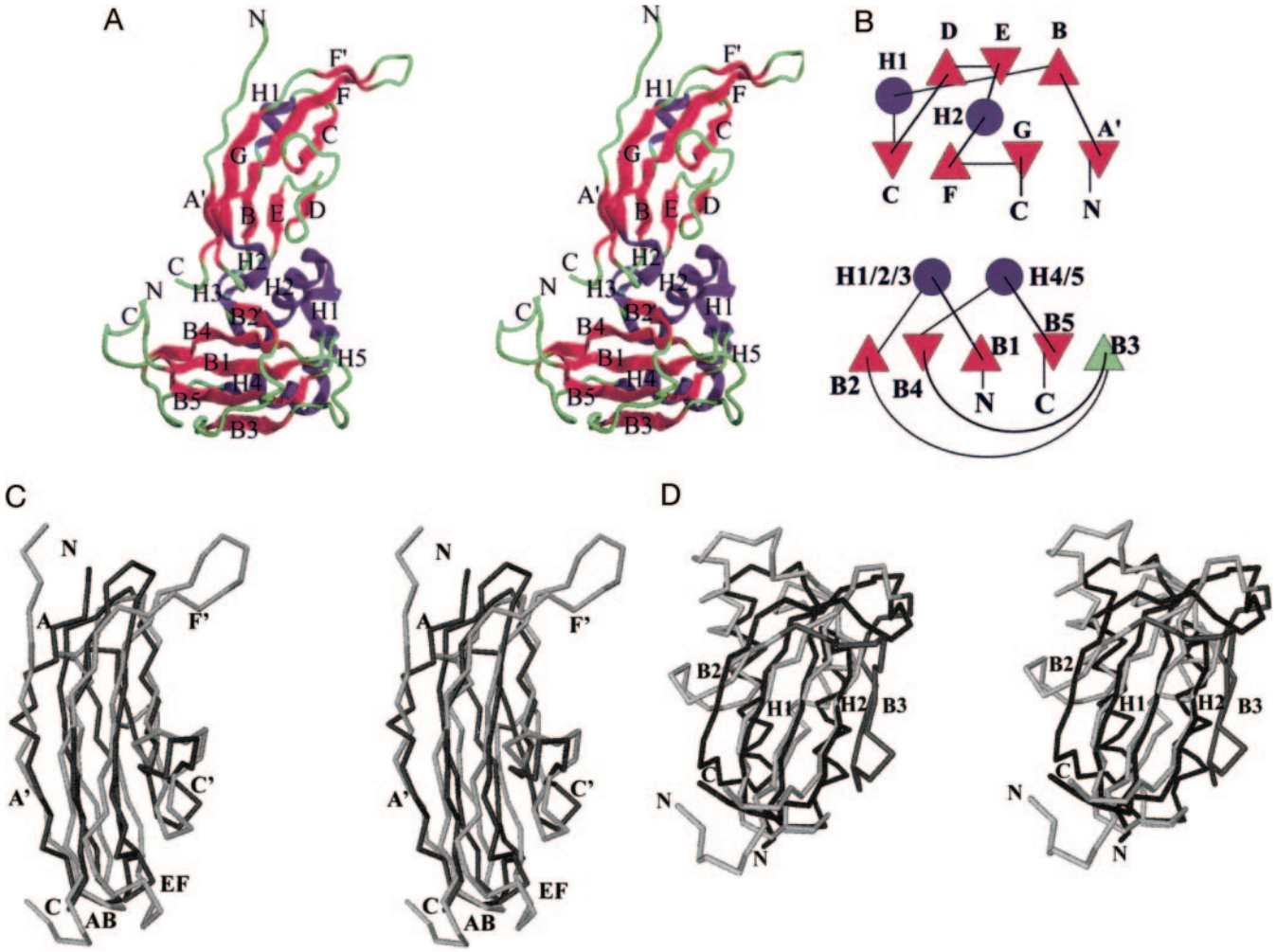

FIG. 2. **Structure and topology of the α-DG N-terminal fragment.** *A*, stereo view of the structure. In domain 1 the structural elements are named according to Harpaz and Chothia (30) and in domain 2 in consecutive order (H for helix and B for β-strand). *B*, topology diagram of the individual domains; helices are shown as *circles* and β-strands as *triangles*. The additional topological element of domain 2 compared with ribosomal protein S6 (25) is shown in *green*. Stereo views of the superimposed structures of the first domain with twitchin (Protein Data Bank entry 1WIT) (*C*) and of the second domain with S6 (Protein Data Bank entry 1RIS) (*D*) are shown.

helices are inserted into this framework; H1 between β-strands B and C and H2 (3_{10} helix) between β-strand E and F.

A DALI search (22) revealed a z-score of 7.0 and an root mean square deviation of 2.4 Å for 78 out of 93 residues with twitchin (23) (Protein Data Bank entry 1WIT) as the closest structural neighbor (Fig. 2*C*). It is noteworthy that the present structure does not confirm a previous prediction, based on multiple sequence alignment, that this domain would show a cadherin-like fold (24).

In contrast to other members of the I-set, the A and C′ strands are not present in the herein described Ig module. The partial de-attachment of the N terminus (Fig. 2, *A* and *C*, and supplemental Fig. 2), and consequently the structural difference to other I-set Ig modules, arises from close crystallographic contacts of the N terminus to the B3B4 connecting loop of domain 2 from a neighboring symmetry related molecule. Another feature of the I-set fold is the conformational conservation of the AB and EF connections (Fig. 2*C*). In α-DG the AB connection fulfils this criterion, whereas the EF connection is longer. A 21-amino acid-long and partially not resolved flexible stretch connects the two domains. The presence of the complete and intact fragment was demonstrated by mass spectrometry using protein from dissolved crystals (data not shown).

The second domain containing residues 180–303 has a ribosomal RNA-binding protein fold (Fig. 2, *A*, *B*, and *D*). The overall dimensions for the second domain are 37 × 30 × 25 Å. It consists of a central five-stranded anti-parallel β-sheet flanked on one side by three helices and leaves the opposite side of the β-sheet exposed and solvent-accessible (Fig. 2, *A* and *D*). An extended loop region between β-strands B2 and B3 folds over the central β-sheet and gives the molecule a "basket"-like shape with the B2B3 connection acting as a "handle." According to DALI (22) the second domain resembles a modification of the ribosomal protein S6 fold (Protein Data Bank code 1RIS) (25). The topology (Fig. 2, *B* and *D*) differs from the S6 fold in the additional B3 β-strand (*green*) with the double crossing of B2B3 and B3B4 interconnecting loops over the central β-sheet as well as the insertion of H1, H3, and the kink in H4H5 helices. This domain was recently identified as a major component of an interaction region between α-DG and the Arena virus GP1 protein (12). Interestingly, within the ribosomal protein S6 and other RNA-binding proteins belonging to the same family, the interactions with RNA have been mapped on the two central β-strands (25). This region corresponds to the B1 and B4 β-strands within a basic cleft of the second domain (Fig. 2*D*).

Interfaces and Crystal Contacts—The interface between domains 1 and 2 (Fig. 3*A*) has a total surface area of ~681 Å^2. A network of close hydrophobic and polar/charged side chain to side chain as well as side chain to backbone, and backbone to

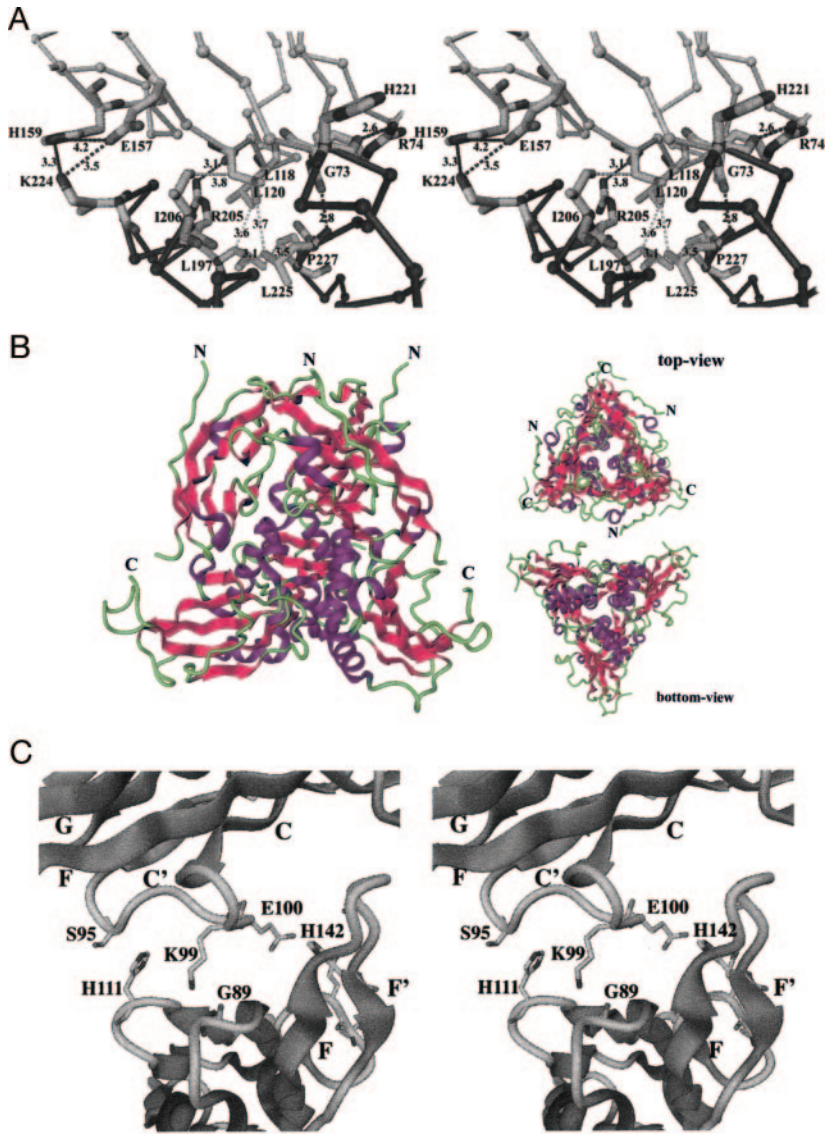

FIG. 3. *A*, stereo view of the domain 1–2 interface. A cluster of hydrophobic residues participating in close contact including Leu^{118}, Leu^{120}, Leu^{197}, Ile^{206}, Leu^{225}, and Pro^{227} are shown. Charged and hydrogen bond interactions are shown in blue. Close interactions are in the range of 2.7–3.5 Å and include residues Gly^{73}, Arg^{74}, Glu^{157}, His^{159}, Leu^{225}, Arg^{205}, Lys^{224}, and Leu^{118}. *B*, view on the crystallographic trimer (*right side*: view from the top/bottom along the 3-fold axis). *C*, stereo view of the CFF′G region of domain 1 forming the trimer interface. Due to close interactions (Lys^{99}-Gly^{89}: 2.8 Å and Glu^{100}-His^{142}: 2.8 Å), the C′ strand gets disrupted and does not adapt to a β-strand conformation.

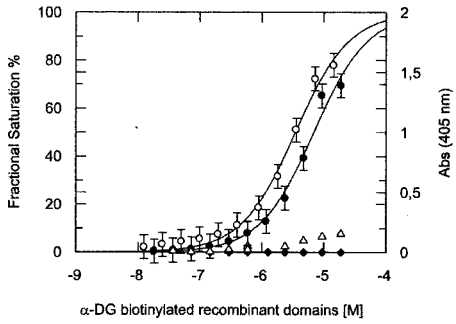

FIG. 4. **Solid-phase binding assays.** The data refer to representative experiments, while the *continuous lines* represent the fitting using a single class of binding site equation as described under "Experimental Procedures." The *bars* indicate the error (≤10%) on each individual absorbance value recorded. Biotinylated α-DG(28–313)R166H (○) and the Ig-like domain 28–168 (●) are able to bind murine laminin-1 in a micromolar concentration range (apparent K_d values are 3.5 ± 2.0 μM and 7.0 ± 1.0 μM, respectively), whereas the 168–313 domain (■) shows a reduced ability to interact with laminin-1. The absence of binding between biotinylated BSA and laminin-1 further indicated the specificity of our observations (♦).

backbone interactions are found. Surface complementarity (26) is 2.9 Å, a value that is in the range of typical antibody-protein and hetero complexes.

The analysis of the crystal packing revealed the presence of a trimer (Fig. 2*B*). The interface is formed by the CFF′G strands including the BC, CD, and DE interconnecting loops and by the H5 helix and surrounding structural elements belonging to domains 1 and 2, respectively (Fig. 3*C*). The major binding contributions arise from the F′G strands and its interconnecting loop pointing into the convex cleft formed by the CFG strands between the FG extension and the CD interconnecting region of a symmetry equivalent molecule. Furthermore, the BC and DE interconnecting loops contact the CD connection of the same symmetry equivalent molecule. Due to this tight association the region that would correspond to the C′-strand, a conserved feature of the I-set of the Ig fold, gets disrupted and does not adapt to a β-strand conformation.

The most prominent interaction of the crystallographic trimer within the second domain is the formation of a trimeric parallel one-heptade-long coiled coil by helix H5 and its symmetry-related counterparts (Fig. 3*B*). Namely, G282, A283, and A286 form the coiled coil interior at positions 1, 2, and 5 of the heptade repeat.

Overall the sum of the three pair-wise interactions bury a total area of about 4300 $Å^2$. This value is well within the range of molecules described to form oligomeric complexes (27). Individual contacts of each domain to the neighboring trimer are in the range of 350 and 120 $Å^2$. However, it is unclear whether

such trimeric assembly could be formed in solution. In fact, sedimentation equilibrium experiments were carried out at increasing concentrations of recombinant α-DG N-terminal fragment (28–313)R166H (up to 0.4 mg/ml) and did not show any self-associating behavior (data not shown).

The Ig-like Domain of α-DG Binds Laminin-1—To investigate whether one of the domains belonging to the N-terminal region is involved in the binding to laminin, we have prepared two new recombinant protein fragments: namely, 28–168 (spanning the Ig-like domain) and 168–313 (spanning the ribosomal domain). Using solid-phase binding assays, we have observed binding (within the low μM range) with coated commercial murine laminin-1 only for the whole N-terminal fragment (28–313)R166H and the Ig-like (28–168) (Fig. 4). Our experiments would confirm the contribution of some protein-protein interactions within the α-DG-laminin complex, as reported recently (13), and show that the binding site for the protein type of interactions to laminin-1 is harbored by the Ig-like domain of α-DG. As a result of the present structural analysis, it is possible that α-DG fragments previously used to perform laminin binding studies could not match the domain borders herein identified (1).

In previous studies, only carbohydrate-mediated binding activities for the interaction between α-DG and its binding partners were described (28). However, the complete exclusion of protein-mediated interactions in such a highly conserved molecule was somehow difficult to understand and justify. It is worth noting that recently it has been reported that the glycosyltransferase LARGE needs to recognize some protein epitopes within the N-terminal region of α-DG to properly initiate its glycosylation (29). The present crystal structure provides the domain boundaries that will help the design of new recombinant constructs to carry out a rational site-directed mutagenesis approach aimed to further investigate important functional aspects of α-DG.

Acknowledgments—We are grateful to Peter Gehrig for help in N-terminal sequencing and mass spectrometric analysis and to Ariel Lustig for sedimentation experiments. We gratefully thank Jürgen Engel for his support and for allowing the continuation of this project outside his group, as well as Markus G. Grütter for providing the scientific environment for the continuation of this project at the University of Zürich.

REFERENCES

1. Ibraghimov-Beskrovnaya, O., Ervasti, J. M., Leveille, C. J., Slaughter, C. A., Sernett, S. W., and Campbell, K. P. (1992) *Nature* **355,** 696–702
2. Smalheiser, N. R., and Schwartz, N. B. (1987) *Proc. Natl. Acad. Sci. U. S. A.* **84,** 6457–6461
3. Cohn, R. D., and Campbell, K. P. (2000) *Muscle Nerve* **23,** 1456–1471
4. Holt, K. H., Crosbie, R. H., Venzke, D. P., and Campbell, K. P. (2000) *FEBS Lett.* **468,** 79–83
5. Brancaccio, A., Schulthess, T., Gesemann, M., and Engel, J. (1995) *FEBS Lett.* **368,** 139–142
6. Tisi, D., Talts, J. F., Timpl, R., and Hohenester, E. (2000) *EMBO J.* **19,** 1432–1440
7. Hohenester, E., Tisi, D., Talts, J. F., and Timpl, R. (1999) *Mol. Cell.* **4,** 783–792
8. Williamson, R. A., Henry, M. D., Daniels, K. J., Hrstka, R. F., Lee, J. C., Sunada, Y., Ibraghimov-Beskrovnaya, O., and Campbell, K. P. (1997) *Hum. Mol. Genet.* **6,** 831–841
9. Cao, W., Henry, M. D., Borrow, P., Yamada, H., Elder, J. H., Ravkov, E. V., Nichol, S. T., Compans, R. W., Campbell, K. P., and Oldstone, M. B. (1998) *Science* **282,** 2079–2081
10. Jung, D., Yang, B., Meyer, J., Chamberlain, J. S., and Campbell, K. P. (1995) *J. Biol. Chem.* **270,** 27305–27310
11. Rambukkana, A., Yamada, H., Zanazzi, G., Mathus, T., Salzer, J. L., Yurchenco, P. D., Campbell, K. P., and Fischetti, V. A. (1998) *Science* **282,** 2076–2079
12. Kunz, S., Sevilla, N., McGavern, D. B., Campbell, K. P., and Oldstone, M. B. (2001) *J. Cell Biol.* **155,** 301–310
13. Hall, H., Bozic, D., Michel, K., and Hubbell, J. A. (2003) *Mol. Cell. Neurosci.* **24,** 1062–1073
14. Bozic, D., Engel, J., and Brancaccio, A. (1998) *Matrix Biol.* **17,** 495–500
15. Otwinowski, Z., and Minor, W. (1997) *Methods Enzymol.* **267,** 307–326
16. Brunger, A. T., Adams, P. D., Clore, G. M., DeLano, W. L., Gros, P., Grosse-Kunstleve, R. W., Jiang, J. S., Kuszewski, J., Nilges, M., Pannu, N. S., Read, R. J., Rice, L. M., Simonson, T., and Warren, G. L. (1998) *Acta Crystallogr. Sect. D Biol. Crystallogr.* **54,** 905–921
17. Collaborative Computational Project Number 4 (1994) *Acta Crystallogr. Sect. D Biol. Crystallogr.* **50,** 760–763
18. de LaFortelle, E., and Bricogne, G. (1997) *Methods Enzymol.* **267,** 472–494
19. Turk, D. (1992) *MAIN*, Technische Universitaet, München, Germany
20. Jones, T. A., Zou, J. Y., Cowan, S. W., and Kjeldgaard, M. (1991) *Acta Crystallogr. Sect. A* **47,** 110–119
21. Sciandra, F., Schneider, M., Giardina, B., Baumgartner, S., Petrucci, T. C., and Brancaccio, A. (2001) *Eur. J. Biochem.* **268,** 4590–4597
22. Holm, L., and Sander, C. (1996) *Science* **273,** 595–603
23. Fong, S., Hamill, S. J., Proctor, M., Freund, S. M., Benian, G. M., Chothia, C., Bycroft, M., and Clarke, J. (1996) *J. Mol. Biol.* **265,** 624–639
24. Dickens, N. J., Beatson, S., and Ponting, C. P. (2002) *Curr. Biol.* **12,** R197–R199
25. Lindahl, M., Svensson, L. A., Liljas, A., Sedelnikova, S. E., Eliseikina, I. A., Fomenkova, N. P., Nevskaya, N., Nikonov, S. V., Garber, M. B., and Muranova, T. A. (1994) *EMBO J.* **13,** 1249–1254
26. Jones, S., and Thornton, J. M. (1996) *Proc. Natl. Acad. Sci. U. S. A.* **93,** 13–20
27. Janin, J., and Rodier, F. (1995) *Proteins* **23,** 580–587
28. Winder, S. J. (2001) *Trends Biochem. Sci.* **26,** 118–124
29. Kanagawa, M., Saito, F., Kunz, S., Yoshida-Moriguchi, T., Barresi, R., Kobayashi, Y. M., Muschler, J., Dumanski, J. P., Michele, D. E., Oldstone, M. B., and Campbell, K. P. (2004) *Cell* **117,** 953–964
30. Harpaz, Y., and Chothia, C. (1994) *J. Mol. Biol.* **238,** 528–539
31. Yeates, T. O. (1997) *Methods Enzymol.* **276,** 344–358

The Structure of the N-terminal Region of Murine Skeletal Muscle α-Dystroglycan Discloses a Modular Architecture

Damir Bozic, Francesca Sciandra, Doriano Lamba and Andrea Brancaccio

J. Biol. Chem. 2004, 279:44812-44816.
doi: 10.1074/jbc.C400353200 originally published online August 23, 2004